Dual-initiation ruptures in the 2024 Mw 7.5 Noto, Japan earthquake encircling a fault asperity at a swarm edge

Liuwei Xu[1], Chen Ji[2], Lingsen Meng[1], Jean-Paul Ampuero[3], Zhang Yunjun[4], Saeed Mohanna[1], Yosuke Aoki[5]

[1]UCLA (xuliuw1997@ucla.edu), [2]UCSB, [3]Geoazur, [4]Chinese Academy of Sciences, [5]University of Tokyo

Abstract

To reveal the connections between the 2024 Mw 7.5 Noto earthquake in Japan and the seismicity swarms that preceded it, we investigated its rupture process through near-source waveform analysis and source imaging techniques, combining seismic and geodetic datasets. We found notable complexity in the initial rupture stages. A strong fault asperity, which remained unbroken in preceding seismic swarms, slowed down the rupture. Then, a second rupture initiated at the opposite edge of the asperity, and the asperity succumbed to double-pincer rupture fronts. The failure of this high-stress drop asperity drove the earthquake into a large-scale event. Our observations help unravel the crucial role of fault asperities in controlling swarm migration and rupture propagation and underscore the need for detailed seismological and interdisciplinary studies to assess seismic risk in swarm-prone regions.

Introduction

The 2024 Noto, Japan earthquake (2024-01-01, Mw 7.5, Figure 1) was well recorded by seismic and geodetic networks at local and teleseismic distances, allowing for in-depth analysis. We investigated the earthquake rupture process by using the slowness-enhanced back-projection (SEBP) and finite fault inversion (FFI) methods to analyze the global and local seismic data, as well as static surface deformation data obtained from global navigation satellite system (GNSS) stations and synthetic-aperture radar (SAR) satellites. We also examined seismic recordings from six nearby stations to unravel the earthquake's intricate early-stage rupture dynamics. Our comprehensive approach provides a detailed characterization of the complex rupture process of the 2024 Noto earthquake.

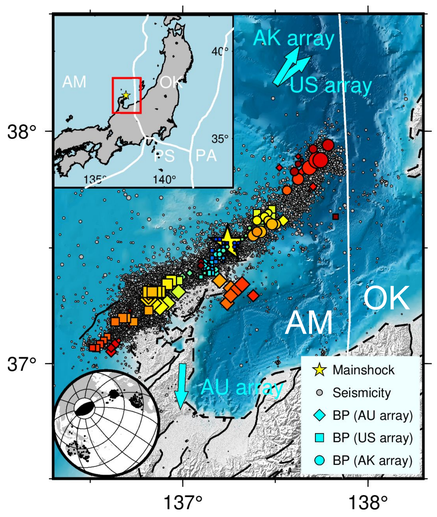

Figure 1: Tectonic map and summary of BP results. The colored symbols denote high-frequency radiators imaged by AU, US, and AK seismic arrays. The symbol size is proportional to the BP energy, and the color represents the rupture time with respect to the mainshock origin time. Gray dots: aftershocks that occurred from 1 to 21 January 2024, JMA. White line: plate boundary between the Amur and Okhotsk plates. AM, Amur plate; OK, Okhotsk plate; PA, Pacific plate; PS, Philippine Sea plate.

Methodology

Slowness-Enhanced Back-Projection (SEBP): teleseismic P waves from Australian (AU), USArray, and Alaskan (AK) arrays (Figure 1); obtain coseismic high-frequency radiators.

Joint Finite Fault Inversion (FFI): teleseismic body and surface waves, local strong motion recordings (Figure 2), local static GNSS recordings (Figure 3), SAR images; obtain coseismic slip distribution and rupture process.

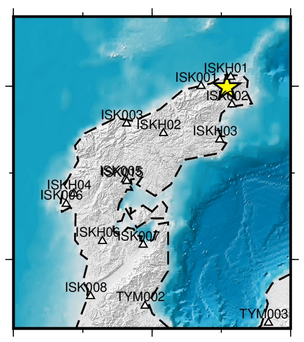

Figure 2: Local strong motion stations used in FFI.

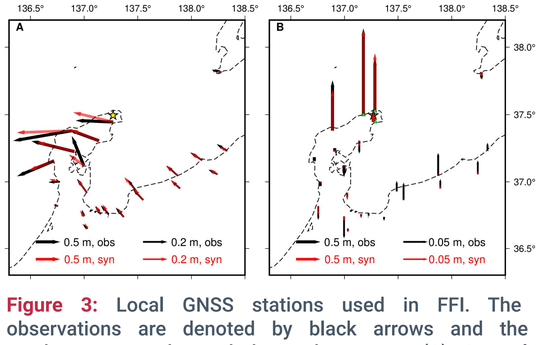

Figure 3: Local GNSS stations used in FFI. The observations are denoted by black arrows and the syntheses are denoted by red arrows. (A) Lateral displacements. (B) Vertical displacements.

Results

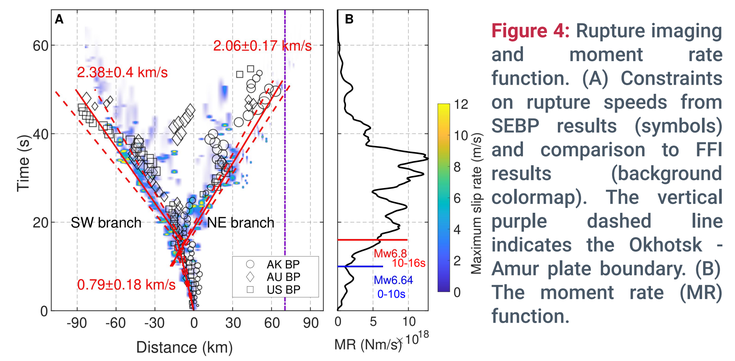

Figure 4: Rupture imaging and moment rate function. (A) Constraints on rupture speeds from SEBP results (symbols) and comparison to FFI results (background colormap). The vertical purple dashed line indicates the Okhotsk - Amur plate boundary. (B) The moment rate (MR) function.

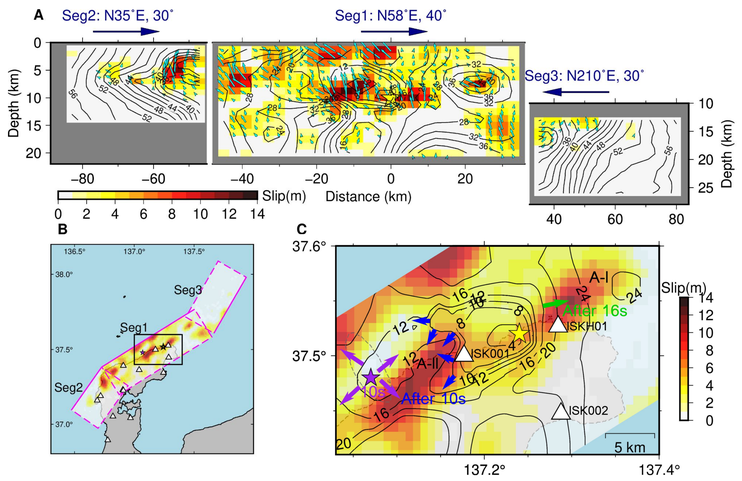

Figure 5: FFI results. (A) Spatial distribution of final slip (colors), rupture initiation time (contours), and slip direction (rake angle, cyan arrows) along the fault system. Top labels: strike and dip angles of each fault segment. (B) Map view of the slip and fault geometry model. The box highlights the source region shown in (C). The white triangles denote strong motion stations. (C) Sketch of the early rupture stage. The yellow star denotes the hypocenter (Hypo-I) and the purple star denotes the second hypocenter (Hypo-II).

Dual-initiation in early rupture

We find remarkable complexity in the initial rupture stages (Figures 5C & 6).
0-8 s: unilateral (SW) rupture from Hypo-I;
8-10 s: the rupture slowed down and almost stopped when reached A-II;
10 s: Hypo-II was triggered and rupture propagated bilaterally;
10-12 s: SW rupture from Hypo-I and NE rupture from Hypo-II encircled A-II;
12-16 s: A-II was broken;
16-50 s: the earthquake developed into Mw 7.5.

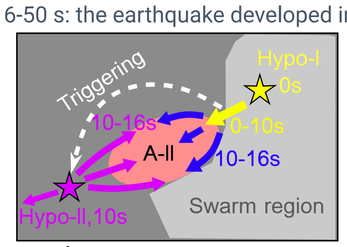

Figure 6: A schematic of the dual initiations and the double-pincer process breaking A-II (Figure 5C). The light gray region denotes the swarm occurrence region before 2024.

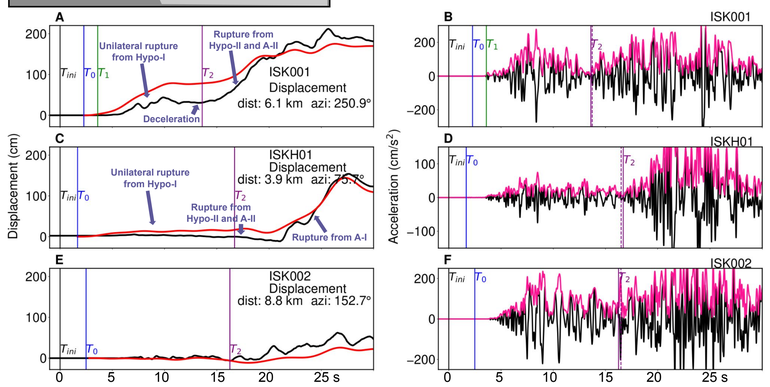

Figure 7: Dual rupture initiations analysis. (A) Vertical displacement (black line) obtained by integrating acceleration recording at station ISK001 (Figure 5C). The red line denotes the predicted waveform by the preferred FFI model. T_{ini}: the earthquake starting time. T_0: the manually picked P arrival, based on (B). T_1: the manually picked beginning of the first wave group, based on (B). T_2 with the solid purple line is the manually picked S arrival in the second wave group. (B) Vertical acceleration seismogram recorded at station ISK001, bandpass filtered to 0.2-5 Hz. The pink line denotes the envelope of the waveform. The dashed purple line is the predicted S arrival time based on the best-fit second hypocenter location. (C,D) The same as (A,B) but for station ISKH01 (Figure 5C). (E,F) The same as (A,B) but for station ISK002 (Figure 5C).

Preceding seismic swarms

Seismic swarms from 2020 to 2023 was organized into four clusters: south (Cluster S), west (Cluster W), north (Cluster N), and east (Cluster E) (Figure 8). The swarm started in late 2020 at Clusters S. About five months later, Cluster W was activated (Figure 8) (Nishimura et al., 2023). The swarm then migrated horizontally to Clusters N and E (Figure 8) (Yoshida et al., 2023). The mainshock initiated within Cluster N (Figure 8). The area near the mainshock hypocenter was seismically inactive until the seismic swarm migrated there in 2021. Within 3 km of the mainshock epicenter, 119 earthquakes of magnitude M≥3 occurred since 2021, including a magnitude 5.4 event in 2022 (Figure 9a) (Yoshida et al., 2023). In contrast, there was no earthquake of magnitude M≥3 from 2000 to 2020 (Figure 9b) (Yoshida et al., 2023 and JMA catalog). Thus, the preceding seismic swarm or its underlying driving process likely led to the nucleation of the 2024 Noto mainshock. The mainshock triggering could be the result of processes such as slow slip (Danré et al., 2024), fluid pressure perturbations (Yoshida et al., 2023), earthquake interactions by stress transfer (Ellsworth & Bulut, 2018), or a combination thereof.

Interestingly, we observe a lack of swarm seismicity before 2024 within A-II (Figure 8), indicating that its behavior as a fault barrier was already apparent during the preceding swarm.

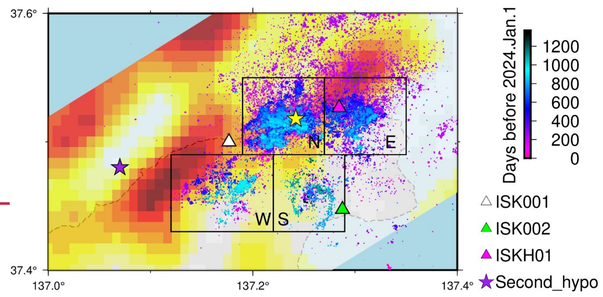

Figure 8: Seismicity between Jan 2020 and Jan 1st, 2024 (Yoshida et al., 2023 and JMA), color-coded by their time relative to the 2024 mainshock. The black boxes and labels indicate the south, west, north, and east swarm clusters. Triangles denote the locations of three strong motion stations, ISK001, ISK002, and ISKH01 (see the legend on the right bottom).

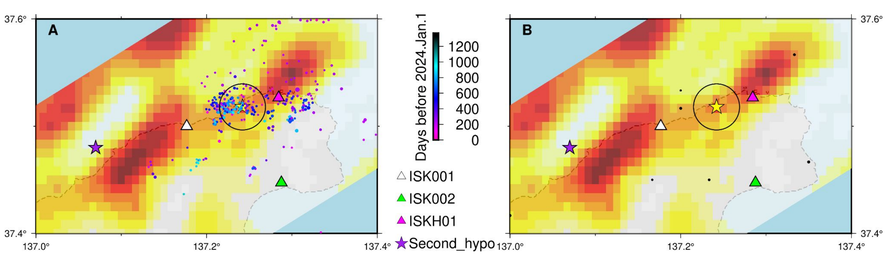

Figure 9: Magnitude 3+ events occurred before 2024 in 3 km epicenter distance range (black open circle) of Hypo-I. (A) The events occurred between Jan 1st, 2021 to Dec 31st, 2023. (B) The events occurred between Jan, 2000 to Dec 31st, 2020.

References

K. Yoshida, N. Uchida, Y. Matsumoto, M. Orimo, T. Okada, S. Hirahara, S. Kimura, R. Hino, Updip fluid flow in the crust of the northeastern Noto Peninsula, Japan, triggered the 2023 Mw 6.2 Suzu earthquake during swarm activity. Geophysical Research Letters, 50, e2023GL106023 (2023).

P. Danré, D. Garagash, L. De Barros, F. Cappa, J.-P. Ampuero, Control of seismicity migration in earthquake swarms by injected fluid volume and aseismic crack propagation. Journal of Geophysical Research: Solid Earth, 129, e2023JB027276 (2024).

T. Nishimura, Y. Hiramatsu, Y. Ohta, Episodic transient deformation revealed by the analysis of multiple GNSS networks in the Noto Peninsula, central Japan. Scientific Report. 13, 8381 (2023).

W.L. Ellsworth, F. Bulut, Nucleation of the 1999 Izmit earthquake by a triggered cascade of foreshocks. Nature Geoscience, 11, 531–535 (2018).

Take a picture to download the full paper

Acknowledgements

This work was funded by a NSF CAREER grant, EAR-1848486 (L.X., L.M., and S.M.), the Leon and Joanne V.C. Knopoff Fund (L.M.), grants from the Southern California Earthquake Center (SCEC), funded by NSF cooperative agreement EAR-0109624 and US Geological Survey (USGS) cooperative agreement 02HQAG0008 (C.J.)